Experimental autoimmune encephalomyelitis disrupts endocannabinoid-mediated neuroprotection

Anke Witting*, Lanfen Chen†‡, Eiron Cudaback*‡, Alex Straiker§, Lisa Walter*¶, Barry Rickman‖, Thomas Möller†**, Celia Brosnan†, and Nephi Stella*†††‡‡§§

Departments of *Pharmacology, §Anesthesiology, ‖Comparative Medicine, **Neurology, ††Psychiatry and Behavioral Sciences, and ‡‡Institute for Stem Cell and Regenerative Medicine, University of Washington, Seattle, WA 98195; and †Department of Pathology, F-520, Albert Einstein College of Medicine, Bronx, NY 10461

Edited by Roger A. Nicoll, University of California, San Francisco, CA, and approved February 14, 2006 (received for review December 5, 2005)

Focal cerebral ischemia and traumatic brain injury induce an escalating amount of cell death because of harmful mediators diffusing from the original lesion site. Evidence suggests that healthy cells surrounding these lesions attempt to protect themselves by producing endocannabinoids (eCBs) and activating cannabinoid receptors, the molecular target for marijuana-derived compounds. Indeed, activation of cannabinoid receptors reduces the production and diffusion of harmful mediators. Here, we provide evidence that an exception to this pattern is found in experimental autoimmune encephalomyelitis (EAE), a mouse model of multiple sclerosis. We show that cell damage induced by EAE does not lead to increase in eCBs, even though cannabinoid receptors are functional because synthetic cannabinoid agonists are known to confine EAE-induced lesions. This lack of eCB increase is likely due to IFN-γ, which is released by primed T cells invading the CNS. We show that IFN-γ disrupts the functionality of purinergic $P2X_7$ receptors, a key step controlling eCB production by microglia, the main source of eCBs in brain. Accordingly, induction of EAE in $P2X_7^{-/-}$ mice results in even lower eCB levels and more pronounced cell damage than in wild-type mice. Our data suggest that the high level of CNS IFN-γ associated with EAE disrupts eCB-mediated neuroprotection while maintaining functional cannabinoid receptors, thus providing additional support for the use of cannabinoid-based medicine to treat multiple sclerosis.

cannabinoid | microglia | purinergic | multiple sclerosis

Physiological stimuli and pathological conditions lead to differential increases in brain endocannabinoids (eCBs) that regulate distinct biological functions. Physiological stimuli lead to rapid and transient (seconds to minutes) increases in eCBs that activate neuronal CB_1 receptors, modulate ion channels, and inhibit neurotransmission (1), whereas pathological conditions lead to much slower and sustained (hours to days) increases in the eCB tone that change gene expression, implementing molecular mechanisms that prevent the production and diffusion of harmful mediators (2–9). Specifically, increases in the eCB tone activate immune CB_2 receptors, which reduce the expression of proinflammatory cytokines and enzymes involved in the generation of free radicals, and neuronal CB_1 receptors, thereby increasing the expression of growth factors. Although we are starting to understand how sustained increases in eCB tone and corresponding activation of cannabinoid receptors implement a protective mechanism to confine lesions, we still lack essential information on the molecular mechanism controlling the brain's eCB tone.

Results

Neuropathologies of different etiologies are all associated with increases in eCB tone (2, 3, 8, 10, 11), suggesting that cell damage itself may initiate this response. In previous studies, we showed that activation of purinergic $P2X_7$ receptors increases the production of the most abundant eCB, 2-arachidonoylglycerol (2-AG), from microglia and that these cells, in conjunction with invading brain macrophages, likely constitute the main source of eCBs in inflamed brain (12–14). These results lead us to hypothesize that the increase in the neuroprotective eCB tone is due to the high concentration of ATP spilled by damaged cells, which activates $P2X_7$ receptors expressed by microglia and invading brain macrophages, enhancing 2-AG production from these cells. Because microglia and invading brain macrophages express $P2X_7$ receptors under experimental autoimmune encephalomyelitis (EAE) conditions (see Fig. 5, which is published as supporting information on the PNAS web site), we sought to test this hypothesis *in vivo* by measuring brain levels of eCBs in areas of marked cell damage in both wild-type (WT) and $P2X_7^{-/-}$ mice. Unexpectedly, we found that brain levels of anandamide and 2-AG were not significantly increased despite the pronounced cell damage induced by EAE (Fig. 1). These results show that contrary to other types of neuropathies, EAE does not lead to a significant increase in eCB tone, suggesting that this autoimmune disease is associated with a step disrupting eCB production. When performing the same experiment in $P2X_7^{-/-}$ mice, we found that brain 2-AG levels were even lower under EAE conditions and axonal damage was more pronounced than in WT mice (Fig. 1). Although these later results agree with the notion that eCB levels determine the extent of cell damage induced by various neuropathies and demonstrate that $P2X_7$ receptors expressed by brain macrophages do control 2-AG levels in inflamed brain, they also suggests that the eCB tone is composed of two components: a $P2X_7$-dependent and a $P2X_7$-independent component, both of which are likely disrupted in EAE-induced damaged area.

EAE is mediated by primed T cells invading the CNS and releasing large amounts of cytokines, including IFN-γ. Local increases in these cytokines skews the phenotype of microglia from being beneficial to detrimental (15). Indeed, upon activation by IFN-γ, microglia produce large amounts of free radicals and proinflammatory cytokines, and few, if any, protective factors. To determine whether IFN-γ tempers the ability of microglia to produce protective eCBs, we treated mouse microglia in primary culture with this cytokine and quantified eCB production by GC/MS. We confirmed that 2-AG levels were increased after the activation of $P2X_7$ receptors by either ATP

Conflict of interest statement: No conflicts declared.

This paper was submitted directly (Track II) to the PNAS office.

Abbreviations: eCB, endocannabinoid; EAE, experimental autoimmune encephalomyelitis; 2-AG, 2-arachidonoylglycerol; $[Ca^{2+}]i$, intracellular calcium concentrations; DG, diacylglycerol; PLC, phospholipase C; MG, monoacylglycerol; Bz-ATP, (benzoylbenzoyl)adenosine triphosphate triethylammonium salt.

See Commentary on page 6087.

‡L.C. and E.C. contributed equally to this work.

¶Present address: Unite d'Immunobiologie des Cellules Dendritiques, Institut Pasteur, 75015 Paris, France.

§§To whom correspondence should be sent at the * address. E-mail: nstella@u.washington.edu.

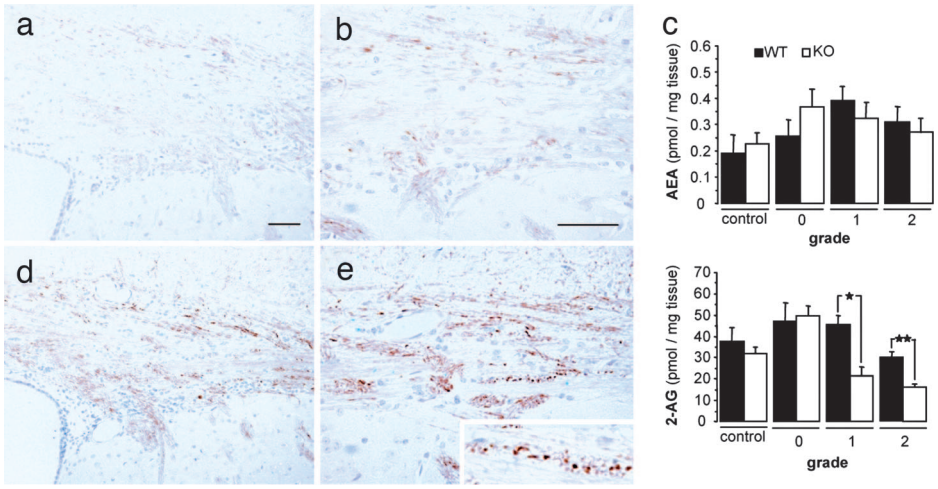

Fig. 1. Lower brain level of 2-AG in $P2X_7^{-/-}$ mice is associated with increased axonal damage induced by EAE. (*a*, *b*, *d*, and *e*) Axonal damage (as assessed by SMI 32 staining) occurring in the choroid plexus (*a* and *d*) and the external capsule (*b* and *e*) of WT (*a* and *b*) and $P2X_7^{-/-}$ (*d* and *e*) mice with EAE (clinical index = grade 2). (Scale bars: 50 μm.) (*c*) Levels of anandamide (AEA) and 2-AG in brain of WT and $P2X_7^{-/-}$ (KO) mice analyzed in control (healthy) animals and in animals with a clinical index of grades 0 (no clinical signs), 1 (flaccid tail), and 2 (hindlimb weakness). Values are mean ± SEM of eCB determination in brain tissues of four to seven mice for each condition. *, $P < 0.05$; and **, $P < 0.01$, significantly different from control (ANOVA) followed by Dunnett's post test).

or (benzoylbenzoyl)adenosine triphosphate triethylammonium salt (Bz-ATP) (14) and found that IFN-γ abolished this response (Fig. 2 *a* and *b*). This effect of IFN-γ was not due to a down-regulation of $P2X_7$ receptor expression, because IFN-γ did not change the overall expression of $P2X_7$ receptors in microglia, nor did it change their expression at the plasma membrane (Fig. 2*c*). These results show that the ability of IFN-γ to disrupt ATP- and Bz-ATP-induced 2-AG production by microglia is not due to the down-regulation of $P2X_7$ receptor expression or disruption of their trafficking to the membrane.

To determine whether IFN-γ affects $P2X_7$ receptor functionality, we performed an electrophysiological characterization of Bz-ATP-induced currents in microglial cells in culture. When applying Bz-ATP to control (untreated) microglia, we found that 8 of 12 cells responded to this ligand (Fig. 3*a*), and 12 of 12 cells responded to this ligand when a low divalent buffer was used [an experimental condition known to potentiate $P2X_7$ responses (16)] (Fig. 3*b*). This result suggests that although all microglia express functional $P2X_7$ receptors, Bz-ATP induces a functional response in only 67% of them under normal divalent ion conditions (17). When performing the same type of experiment on IFN-γ-treated microglia, we found that no cells (0/12) responded to Bz-ATP under normal divalent ion conditions, but they all did under low divalent ion conditions (Fig. 3*c*). This result shows that all IFN-γ-treated cells do express $P2X_7$ receptors, but none of these receptors are functional under normal divalent ion conditions.

Increases in 2-AG production require a long-lasting rise in intracellular calcium concentrations ($[Ca^{2+}]i$), and engagement of $P2X_7$ receptors leads to such a response (14). Thus, we used fura-2 imaging to determine whether IFN-γ disrupts the $P2X_7$ receptor-induced rise in $[Ca^{2+}]i$. As previously shown in control microglia, ATP induced a biphasic rise in $[Ca^{2+}]i$: a rapid and transient rise in $[Ca^{2+}]i$ (due to P2Y receptor-induced release of calcium from intracellular stores) and a more sustained rise in $[Ca^{2+}]i$ (due to $P2X_7$ receptor-induced influx of extracellular calcium) (Fig. 3*d*). In line with this result, activation of $P2X_7$ receptors with Bz-ATP only induced the sustained rise in $[Ca^{2+}]i$ (Fig. 3*e*). We found that IFN-γ selectively prevented the second rise in $[Ca^{2+}]i$ induced by ATP and Bz-ATP (Fig. 3 *d* and *e*). Together with our electrophysiological data, these results show that IFN-γ disrupts $P2X_7$ receptor functionality and associated calcium influx, an effect that could account for the lower 2-AG tone measured in the brains of EAE mice.

To determine whether the effect of IFN-γ on 2-AG production was specific to $P2X_7$ receptors or whether it could be extended to $P2X_7$-independent stimuli, we tested the effect of IFN-γ on 2-AG production induced by two receptor-independent stimuli: the calcium ionophore ionomycin and the diacylglycerol (DG) kinase inhibitor DGKI1 (14). Both agents increased 2-AG production in a calcium- and IFN-γ-dependent manner (Fig. 3*f*), suggesting that IFN-γ also affects one or more enzymatic steps involved in 2-AG production, such as phospholipase C (PLC), DG lipase and/or monoacylglycerol (MG) lipase (14). Although IFN-γ did not affect PLC and MG lipase activities (Table 1 and Fig. 4 *c* and *d*), it decreased DG lipase activity by selectively reducing the mRNA expression of DG lipase α, one of the two isotypes recently shown to mediate 2-AG production (18) (Fig. 4 *a* and *b*).

Our results outline a mechanism by which localized increases in IFN-γ associated with EAE is likely to disrupt 2-AG-mediated neuroprotection. Initial EAE-induced cell damage leads to the activation of resident microglia and recruitment of macrophages, inducing $P2X_7$ receptor expression in these cells. The large number of primed T cells invading the CNS and releasing IFN-γ disrupts $P2X_7$ receptor functionality and reduces DG lipase expression, thus preventing the increase in 2-AG tone that should have been initiated by the high concentration of ATP spilled by damaged cells. Such a disruption in 2-AG protection leaves surrounding cells vulnerable to further damage. Here six points are noteworthy. (*i*) Although rapid and transient increases in eCB levels are controlled by on–off synaptic transmission, slower changes in eCB tone are likely controlled by mediators that remain elevated for longer periods of time. ATP spilled by damaged cells fulfills this criterion (13). (*ii*) The protective role of $P2X_7$ receptors in EAE contrasts with their detrimental role in arthritis and spinal cord injury and their lack of involvement in cerebral ischemia (19, 20). (*iii*) The fact that genetic deletion of $P2X_7$ receptors leads to even lower levels of 2-AG and exacerbates cell damage supports the notion that 2-AG levels determine the extent of lesions occurring under neuropathological conditions (3). (*iv*) The slight 2-AG protective tone that remains in WT mice undergoing EAE is likely due to resident microglial cells distant from primed T cells. (*v*) The selective

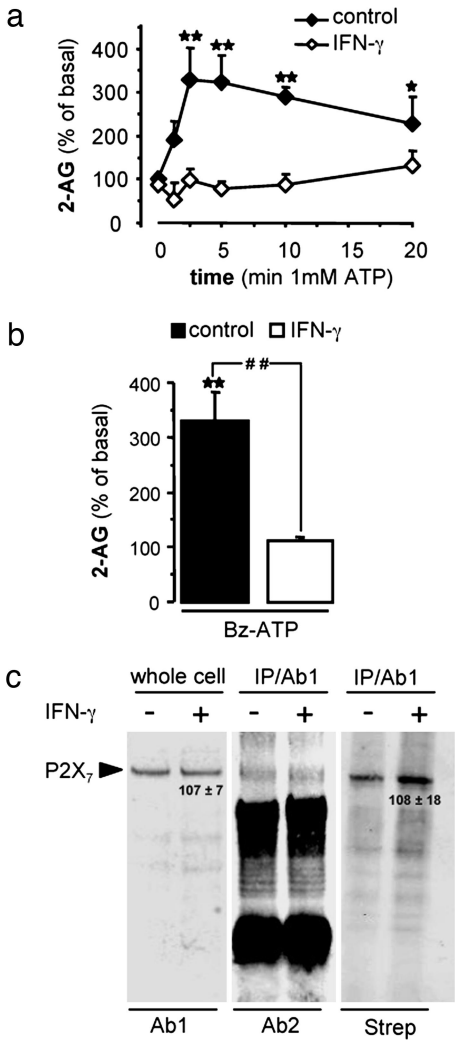

Fig. 2. IFN-γ disrupts the $P2X_7$-mediated production of 2-AG by microglia in primary culture without affecting receptor expression. (*a* and *b*) Microglial cells were treated 18–24 h with vehicle (control) or 100 units/ml IFN-γ and then incubated with vehicle (basal) or ATP (1 mM) for increasing periods of time (*a*) or with Bz-ATP (200 μM) for 10 min (*b*), and eCBs were quantified. Values are mean ± SEM of independent eCB quantifications, each performed on one 60-mm dish of cells ($n = 6–88$ dishes: i.e., 3–44 separate experiments performed in duplicate). *, $P < 0.05$, and **, $P < 0.01$, significantly different from basal (ANOVA followed by Dunnett's post test). Anandamide (AEA) remained below detection limit throughout the incubation period (data not shown) and in both control and IFN-γ treated cells. Basal 2-AG levels in untreated and IFN-γ-treated microglia were 8.7 ± 1.2 pmol/mg protein ($n = 133$) and 10.4 ± 2.1 pmol/mg protein ($n = 25$), respectively ($P > 0.05$ when compared with Student's *t* test). (*c*) Microglial cells were treated 18–24 h with vehicle (control) or 100 units/ml IFN-γ and analysis by Western blot. Representative blot showing whole-cell lysate probed with $P2X_7$ Ab #1 (Ab1; Santa Cruz Biotechnology) (*Left*), whole-cell lysate immunoprecipitated with $P2X_7$ Ab #1 (IP/AB1) and probed with $P2X_7$ Ab #2 (AB2; Alomone Labs) (*Center*), and biotin-labeled membrane fractions immunoprecipitated with $P2X_7$ Ab #1 (IP/AB1) probed with streptavidin (Strep) (*Right*). Numbers show average optic density from three independent experiments, expressed as percent of untreated (−) cells.

disruption of 2-AG tone found in EAE vs. the increase in 2-AG tone found in traumatic brain injury, excessive seizures, and SODG93A-induced degeneration (10, 11) likely reflects the involvement of primed T cells in EAE pathogenesis, but not in the other models. (*vi*) Finally, Baker *et al.* (21) reported a small, but significant, increase in brain and spinal cord levels of anandamide and 2-AG in mice with EAE, compared with their controls. Our results likely differ from those of Baker *et al.* (21) because this group used a mouse model of multiple sclerosis not associated with immune cell infiltration (acute spastic) and thus not involving IFN-γ.

In conclusion, our results, together with studies showing that cannabinoid agonists or inhibitors of eCB inactivation temper EAE pathogenesis (21–26), suggest that IFN-γ does not affect CB receptor signaling and thus provide further support for using cannabinoid-based agents for treatment of multiple sclerosis (27, 28).

Materials and Methods

ADP, ATP, adenosine 5′-triphosphate-2′,3′-dialdehyde (oxidized ATP), Bz-ATP, DGKI1, and EGTA were purchased from Sigma. Recombinant mouse IFN-γ and ionomycin were from Calbiochem. PRIMERIA tissue culture dishes and well plates were purchased from VWR International. CellGro (Complete serum free cell culture medium) was purchased from Mediatech (Washington, DC).

EAE Induction and eCB Analysis. $P2X_7^{-/-}$ mice back-crossed for 12 generations to C57BL/6 mice were kindly supplied by Christopher A. Gabel (Pfizer). C57BL/6 mice were obtained from the same source (Taconic Farms). Successful truncation of the $P2X_7$ receptor was confirmed by PCR (primer sequences used for WT; 5′-GCA GCC CAG CCC TGA TAC AGA CAT T-3′ and 5′-TCG GGA CAG CAC GAG CTT ATG GA-3′; for the KO, 5′-GAC AGC CCG AGT TGG TGC CAG TGT G-3′ and 5′-GGT GGG GGT GGG GGT GGG ATT AGA T-3′). All animals were housed and maintained in a federally approved animal facility, and the Animal Care and Use Committee of Albert Einstein College of Medicine approved all protocols. EAE was induced in mice (at 7–9 weeks) with 300 μg of myelin oligodendrocyte glycoprotein (MOG) $peptide_{35–55}$ (MEVGWYRSPFSRVVHLYRNGK, Celtek Bioscience, Nashville, TN). EAE was scored as follows: 0, no clinical signs; 1, flaccid tail; 2, hindlimb weakness; 3, hindlimb paralysis; 4, forelimb and hindlimb paralysis; 5, death. Slices (10 mg) were sectioned, and eCB therein was analyzed as described in ref. 11.

Immunocytochemistry. Immunostaining was performed on 5 μm of fresh frozen (acetone fixed) sections by using a rabbit polyclonal antibody (Ab) against the mouse $P2X_7$ receptor (1:500; Alomone Labs, Jerusalem), a rat anti-mouse F4/80 monoclonal Ab (1:50, Serotec), and a secondary IgG Ab conjugated with Alexa 488 and 594 (1:200; JacksonImmuno Research). Images were acquired with a Leica TCS SP/NT confocal microscope (Keck Center, University of Washington). Nonspecific staining was determined with parallel immunostaining experiments performed in the presence of the appropriate immunizing antigen and using equal gain settings during acquisition and analysis.

SMI-32 staining was performed by using paraffin-embedded sections. Samples were deparaffinized, boiled for antigen retrieval in sodium citrate buffer (DAKO) for 20 min, incubated with 3% H_2O_2 for 30 min, and blocked in PBS containing 10% normal goat serum and 0.05 mg/ml purified rat anti-mouse CD16/CD32 monoclonal Ab for 1 h at room temperature (RT). Tissues were stained overnight at 4°C with the SMI-32 Ab (1:1,000; Sternberger Monoclonals, Berkeley, CA) in 5% normal goat serum/PBS. After washing twice in PBS, horseradish peroxidase-conjugated goat anti-mouse IgG was applied for 2 h at RT, and samples were developed by using the ABC method with diaminobenzidine (Vectastain; Vector Laboratories).

Cell Culture and Incubation, Lipid Extraction, and eCB Analysis. Mouse microglial cells in primary cultures were prepared as described in ref. 14, according to the guidelines of the Institutional Animal

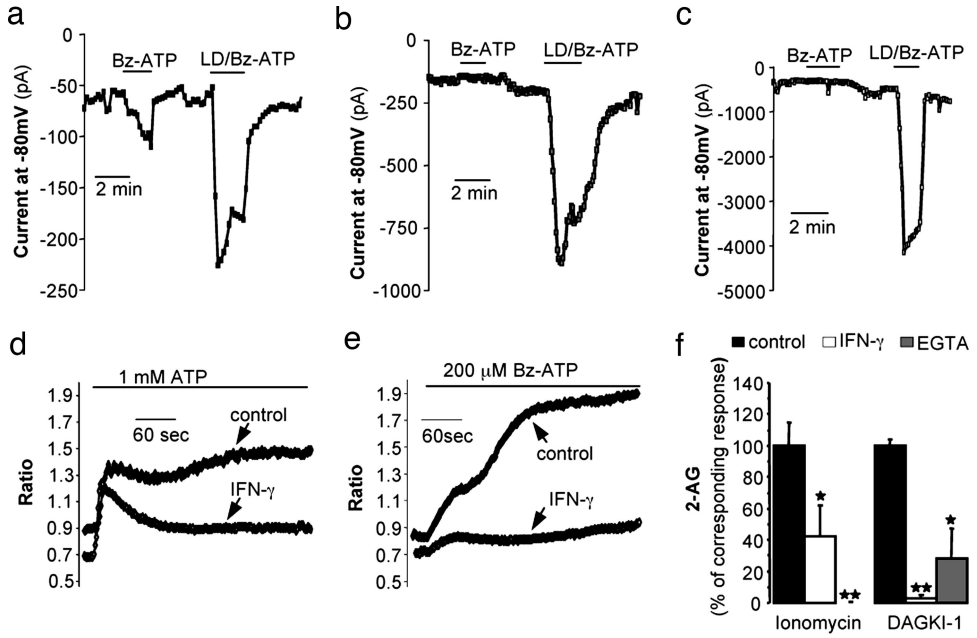

Fig. 3. IFN-γ disrupts the functionality of $P2X_7$ receptors and an enzymatic step involved in 2-AG production. (*a–c*) Representative current induced by Bz-ATP (200 μM) in normal buffer (Bz-ATP) and in low divalent buffer (LD/Bz-ATP) in a responding control microglia (*a*), a nonresponding control microglia (*b*), and IFN-γ-treated microglia (*c*) (all at a holding potential of −80 mV). Mean induced currents were as follows: responding control microglia, −401 ($n = 6$); nonresponding control microglia, −132 ($n = 6$); control microglia in low divalent buffer, −1,419 ($n = 4$); IFN-γ-treated microglia, −150 ($n = 7$); IFN-γ-treated microglia in low divalent buffer, −1,777 ($n = 4$). Mean resting membrane potential were as follows: responding control microglia, −45.8 ($n = 8$); nonresponding control microglia, −28.1 ($n = 4$); and IFN-γ-treated microglia, −20.9 ($n = 12$). (*d* and *e*) $[Ca^{2+}]i$ in microglia treated 18–24 h with vehicle (control) or 100 units/ml IFN-γ and then perfused with ATP (1 mM) (*d*) and Bz-ATP (200 μM) (*e*). Ratio plots were averages from ≈25 cells analyzed in the field of view and are representative of three independent experiments. (*f*) 2-AG levels in microglia treated 18–24 h with vehicle (control) or 100 units/ml IFN-γ, then preincubated for 30 min with vehicle or EGTA (1 mM) before incubation with ionomycin (5 μM) or DAGK1 (30 μM) for 5 min, and eCB quantification by GC/MS. Values are mean ± SEM of independent eCB quantifications, each performed on one 60-mm dish of cells ($n = 6–12$ dishes: i.e., 3–6 separate experiments performed in duplicate). *, $P < 0.05$, and **, $P < 0.01$, significantly different from basal (ANOVA followed by Dunnett's post test).

Care and Use Committee of the University of Washington. Cells were rinsed once with HB buffer (20 mM Hepes/5 mM $NaHCO_3$/120 mM NaCl/5 mM KCl/2 mM $CaCl_2$/1 mM $MgSO_4$/1 mM NaH_2PO_4/10 mM glucose, pH 7.4) and placed on a shaking water bath at 37°C for a 30-min preincubation time period. Cells then were stimulated by directly adding agents prepared at 10× in HB buffer and incubated for an additional 10 min; placing dishes on ice and adding ice-cold methanol stopped incubations. Lipids were extracted with chloroform containing internal standards (200 pmol of $[^2H_4]$eCB). Organic phases were purified by open-bed silica gel chromatography followed by high-performance liquid chromatography (HPLC), and eCB amounts were determined by chemical ionization-GC/MS by using isotope dilution as a quantification method.

Western Blot and Immunoprecipitation. Whole-cell lysates were electrophoresed (SDS/PAGE), transferred to poly(vinylidene fluoride), and immunoblotted by using Ab directed against the $P2X_7$ receptor (1:1,000; Santa Cruz Biotechnology). For detection of $P2X_7$ receptor expression at the cell surface, primary microglia were treated with vehicle or IFN-γ for 18 h, washed, and incubated with biotin (EZ-Link Sulfo-NHS-LC-Biotin; Pierce) for 30 min. $P2X_7$ receptors were immunoprecipitated from biotinylated lysates by using the same Ab, electrophoretically separated, blotted, and probed with streptavidin. Specificity of the immunoprecipitating Ab was assessed by using Western blot analysis and a second anti-$P2X_7$ Ab (Alomone Labs).

Table 1. IFN-γ does not affect PLC activity in microglia

	PLC activity, % of basal	
Conditions	Control	IFN-γ
Basal	100 ± 2	100 ± 3
ADP	200 ± 9	229 ± 9
Ionomycin	178 ± 5	192 ± 17

Microglia were incubated with either vehicle or IFN-γ (100 units/ml for 18 h), stimulated with ADP (300 μM for 10 min) or ionomycin (5 μM for 5 min), and $[^3H]$IP production was determined. Values are mean ± SEM of 9–38 determinations of radioactivity (i.e., 3–19 separate experiments performed in triplicate).

Electrophysiological Recordings. Currents were recorded by using the whole-cell voltage-clamp technique. Briefly, cells were perfused (1–2 ml/min) with HB buffer. Data were digitized and recorded by using PULSE (HEKA Elektronics, Lambrecht/Pfalz, Germany) software in conjunction with an Axopatch 200A amplifier (Axon Instruments, Union City, CA), and the data were analyzed by using an in-house VISUAL BASIC (Microsoft) analysis program. Liquid junction potentials were determined experimentally to be −8 mV and were uncorrected. For measuring currents, the pipette solution contained 121.5 mM K-gluconate, 10 mM Hepes, 17 mM KCl, 9 mM NaCl, 1 mM $MgCl_2$, 0.2 mM EGTA, 2 mM MgATP, and 0.5 mM LiATP (pH 7.2) with KOH. Low divalent external solutions consisted of HB buffer containing 0.09 mM $CaCl_2$ and no $MgCl_2$. Measured current was defined as that portion of the current elicited at −80 mV by a ramping voltage stimulus (−100 to +35 mV; 0.54 mV/sec; holding potential −70 mV). Resting membrane potential was measured both by means of the ramping protocol (owing to the lack of voltage-activated currents) and by manually zeroing out the holding current. As a rule the two values were in

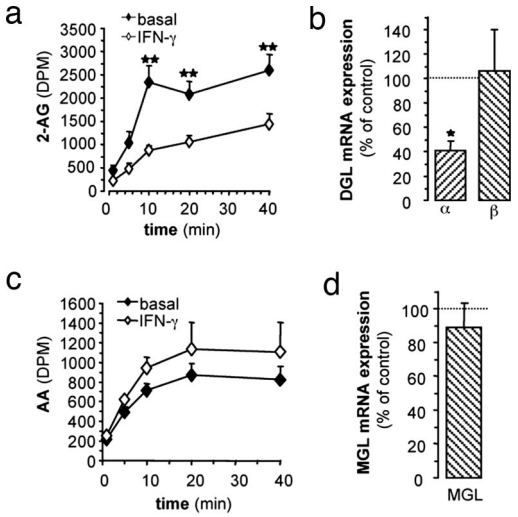

Fig. 4. IFN-γ selectively lowers the expression of DG lipase α in microglia. (*a* and *b*) DG and MG lipase activities were measured by providing [^{14}C]DG (*a*) or [^{14}C]2-AG (*b*) to whole-cell lysate prepared from untreated and IFN-γ-treated microglia in primary culture (100 units/ml for 18–24 h). At specific time points, lipids were chloroform-extracted and separated by thin-layer chromatography, bands with the same retention time as 2-AG (*a*) or arachidonic acid (AA) (*c*) were scraped off, and the radioactivity therein was determined by liquid scintillation. Values are mean ± SEM of 6–14 independent determinations of radioactivity (three to seven separate experiments performed in duplicate). (*b* and *d*) Quantitative RT-PCR showing mRNA levels of DG lipase (DGL) α and β (*b*) and MG lipase (MGL) (*d*). Dotted line represents levels of mRNA found in untreated microglia, and values are expressed in percent of this control and correspond to mean ± SEM of three determinations in IFN-γ-treated microglia (100 units/ml for 18–24 h).

close agreement and were averaged to produce a final value. Currents were sampled at 5 kHz. To control for possible variations of response from given cultured plates, measures were obtained from three separate cultures. In addition, to avoid one source of systemic bias, experimental and control measures were alternated whenever possible, and concurrent controls were always performed.

Calcium Imaging. Calcium imaging was performed as described in ref. 14. Briefly, cells were incubated with fura-2-acetoxymethyl ester (Molecular Probes) (5 μM) for 30 min and placed in a perfusion chamber on the stage of an inverted microscope (Diaphot 200; Nikon) equipped with a 40×/1.3 numerical aperture oil immersion objective. Fura-2 was excited by using a Lambda DG-4 filter system (Sutter Instruments, Novato, CA) at 340 and 380 nm, and fluorescence emission was collected at 510 ± 20 nm via a bandpass filter. Acquisition of fluorescence and image analysis was performed by using a digital imaging system (R3; Inovision, Durham, NC). Ratios were collected at time intervals of 2 sec. Drugs were added to the chamber under nonperfused conditions, so that these conditions were similar to those used for analyzing eCB production.

PLC Activity. PLC activity was determined as described in ref. 14. Briefly, cells were incubated with myo-[^{3}H]inositol [4 μCi/ml (0.2 nmol) for 18 h; American Radiolabeled Chemicals, St. Louis], rinsed, and preincubated and incubated with HB buffer containing lithium chloride (10 mM). Incubation was stopped with Triton X-100, and radioactive lipids were isolated with methanol/chloroform (1:2 vol/vol) and loaded onto Dowex AG 1 × 8 columns (formate form, 200–400 mesh; Bio-Rad). [^{3}H]IP were eluted with ammonium formate/formic acid, and radioactivity was determined.

DG and MG Lipase Activity. DG and MG lipase activity was determined as described in ref. 14. Briefly, cell homogenates (35 μg of protein final) were incubated with [^{14}C]DG [9 nCi/ml (0.18 nmol); Amersham Pharmacia Biotech] or [^{3}H]2-AG [15 nCi/ml (0.075 pmol); American Radiolabeled Chemicals]. Adding methanol stopped the incubation, and lipids were extracted with chloroform containing 15 μM DG, 2-AG, and AA. Samples were separated by thin-layer chromatography, lipids were visualized with phosphomolybdic acid, bands were scraped off, and radioactivity therein was determined by liquid scintillation.

Real-Time PCR. Samples were homogenized in TRIzol reagent (Invitrogen Life Technologies), and total RNA was extracted by using RNeasy (Qiagen, Valencia, CA). QRT-PCR was performed by using SYBR Green Q-PCR Master Mix (Applied Biosystems), with acidic ribosomal binding protein (ARBP) acting as an internal control gene. Primers were as follows: ARBP, forward, 5′-GGTGTTTGACAACGACAGCATT-3′, and reverse, 5′-CAGGGCCTGCTCTGTGATGT-3′; MGL, forward, 5′-CTGCAACACGTGGACACCAT-3′, and reverse, 5′-GAGTGGCCCAGGAGGAAGA-3′; DGLα, forward, 5′-CCGCACCTTCGTCAAGCT-3′, and reverse = 5′ CGGTGCCGCAGGTTGTA-3′; DGLβ, forward, 5′-GCTCAAGCGGCCAGATACAT-3′, and reverse, 5′-CACTGAAGGCTTGGCTCAGAA-3′. Corresponding cycle threshold (*ct*) values were normalized by using a Δ*ct*-based algorithm ($ct_{GPR55} - ct_{ARBP}$), yielding arbitrary units that represent relative expression levels between samples.

We thank Dr. Ken Mackie for support. This work was supported by the National Institute on Drug Abuse (to N.S. and Ken Mackie) and the National Institute of Neurological Disorders and Stroke (to T.M. and C.B.).

1. Freund, T. F., Katona, I. & Piomelli, D. (2003) *Physiol. Rev.* **83,** 1017–1066.
2. Franklin, A., Parmentier-Batteur, S., Walter, L., Greenberg, D. A. & Stella, N. (2003) *J. Neurosci.* **23,** 7767–7775.
3. Panikashvili, D., Simeonidou, C., Ben-Shabat, S., Hanus, L., Breuer, A., Mechoulam, R. & Shohami, E. (2001) *Nature* **413,** 527–531.
4. Wallace, M. J., Blair, R. E., Falenski, K. W., Martin, B. R. & DeLorenzo, R. J. (2003) *J. Pharmacol. Exp. Ther.* **307,** 129–137.
5. Nagayama, T., Sinor, A. D., Simon, R. P., Chen, J., Graham, S. H., Jin, K. & Greenberg, D. A. (1999) *J. Neurosci.* **19,** 2987–2995.
6. Stella, N. (2004) *Glia* **48,** 267–277.
7. Parmentier-Batteur, S., Jin, K., Ou Mao, X., Xie, L. & Greenberg, D. A. (2002) *J. Neurosci.* **22,** 9771–9775.
8. Marsicano, G., Goodenough, S., Monory, K., Hermann, H., Eder, M., Cannich, A., Azad, S. C., Grazia Cascio, M., Ortega Gutiérrez, S., Van der Stelt, M., *et al.* (2003) *Science* **302,** 84–88.
9. Klegeris, A., Bissonnette, C. J. & McGeer, P. L. (2003) *Br. J. Pharmacol.* **139,** 775–786.
10. Ferrer, B., Asbrock, N., Kathuria, S., Piomelli, D. & Giuffrida, A. (2003) *Eur. J. Neurosci.* **18,** 1607–1614.
11. Witting, A., Weydt, P., Hong, S., Kliot, M., Moller, T. & Stella, N. (2004) *J. Neurochem.* **89,** 1555–1557.
12. Walter, L., Franklin, A., Witting, A., Wade, C., Xie, Y., Kunos, G., Mackie, K. & Stella, N. (2003) *J. Neurosci.* **23,** 1398–1405.
13. Wang, X., Arcuino, G., Takano, T., Lin, J., Peng, W. G., Wan, P., Li, P., Xu, Q., Liu, Q. S., Goldman, S. A. & Nedergaard, M. (2004) *Nat. Med.* **10,** 821–827.
14. Witting, A., Walter, L., Wacker, J., Moller, T. & Stella, N. (2004) *Proc. Natl. Acad. Sci. USA* **101,** 3214–3219.
15. Juedes, A. E., Hjelmstrom, P., Bergman, C. M., Neild, A. L. & Ruddle, N. H. (2000) *J. Immunol.* **164,** 419–426.
16. Surprenant, A., Rassendren, F., Kawashima, E., North, R. A. & Buell, G. (1996) *Science* **272,** 735–739.
17. Bianco, F., Fumagalli, M., Pravettoni, E., D'Ambrosi, N., Volonte, C., Matteoli, M., Abbracchio, M. P. & Verderio, C. (2005) *Brain Res. Brain Res. Rev.* **48,** 144–156.

18. Bisogno, T., Howell, F., Williams, G., Minassi, A., Cascio, M. G., Ligresti, A., Matias, I., Schiano-Moriello, A., Paul, P., Williams, E. J., *et al.* (2003) *J. Cell Biol.* **163,** 463–468.
19. Labasi, J. M., Petrushova, N., Donovan, C., McCurdy, S., Lira, P., Payette, M. M., Brissette, W., Wicks, J. R., Audoly, L. & Gabel, C. A. (2002) *J. Immunol.* **168,** 6436–6445.
20. Le Feuvre, R., Brough, D. & Rothwell, N. (2002) *Eur. J. Pharmacol.* **447,** 261–269.
21. Baker, D., Pryce, G., Croxford, L. J., Brown, P., Pertwee, R. G., Makriyannis, A., Knanolkar, A., Layward, L., Fezza, F., Bisogno, T. & DiMarzo, V. (2001) *FASEB J.* **15,** 300–302.
22. Cabranes, A., Venderova, K., de Lago, E., Fezza, F., Sanchez, A., Mestre, L.,Valenti, M., Garcia-Merino, A., Ramos, J. A., Di Marzo, V. & Fernandez-Acenero, M. J. (2005) *Neurobiol. Dis.* **20,** 207–217.
23. Mestre, L., Correa, F., Arevalo-Martin, A., Molina-Holgado, E., Valenti, M., Ortar, G., Di Marzo, V. & Guaza, C. (2005) *J. Neurochem.* **92,** 1327–1339.
24. Croxford, J. L. & Miller, S. D. (2003) *J. Clin. Invest.* **111,** 1231–1240.
25. Baker, D., Pryce, G., Croxford, L. J., Brown, P., Pertwee, R. G., Huffman, J. W. & Layward, L. (2000) *Nature* **404,** 84–87.
26. Arévalo-Martín, Á., Vela, J. M., Molina-Holgado, E., Borrell, J. & Guaza, C. (2003) *J. Neurosci.* **23,** 2511–2516.
27. Pertwee, R. G. (2002) *Pharmacol. Ther.* **95,** 165–174.
28. Pryce, G. & Baker, D. (2005) *Trends Neurosci.* **28,** 272–276.